Lawrence Berkeley National Laboratory

LBL Publications

Title

Oxidative footprinting in the study of structure and function of membrane proteins: current state and perspectives.

Permalink

https://escholarship.org/uc/item/7tt34708

Journal

Biochemical Society Transactions, 43(5)

ISSN

0300-5127

Authors

Bavro, Vassiliy N

Gupta, Sayan

Ralston, Corie

Publication Date

2015-10-01

DOI

10.1042/bst20150130

Peer reviewed

eScholarship.org Powered by the California Digital Library
University of California

Oxidative footprinting in the study of structure and function of membrane proteins: current state and perspectives

Vassiliy N. Bavro[1*], Sayan Gupta[2,3], Corie Ralston[3]

[1]*Institute of Microbiology and Infection, School of Immunity and Infection, University of Birmingham, Birmingham, B152TT, UK*
[2]*Center for Proteomics and Bioinformatics, Case Western Reserve University, Ohio, US*
[3]*Berkeley Center for Structural Biology, Lawrence Berkeley National Laboratory, California, US*

**to whom correspondence should be addressed : v.bavro@bham.ac.uk*

Abstract: Membrane proteins, such as receptors, transporters and ion channels control the vast majority of cellular signaling and metabolite exchange processes and thus are becoming key pharmacological targets. Obtaining structural information by usage of traditional structural biology techniques is limited by the requirements for the protein samples to be highly pure and stable when handled in high concentrations and in non-native buffer systems, which is often difficult to achieve for membrane targets. Hence, there is a growing requirement for the use of hybrid, integrative approaches to study the dynamic and functional aspects of membrane proteins in physiologically relevant conditions. In recent years, significant progress has been made in the field of oxidative labeling techniques, and in particular the X-ray radiolytic footprinting in combination with mass spectroscopy (XF-MS), which provide residue-specific information on the solvent accessibility of proteins. In combination with both low- and high-resolution data from other structural biology approaches it is capable of providing valuable insights into dynamics of membrane proteins, which have been difficult to obtain by other structural techniques, proving a highly complementary technique to address structure and function of membrane targets. XF-MS has demonstrated a unique capability for identification of structural waters and conformational changes in proteins at both a high degree of spatial and temporal resolution. Here, we provide a perspective on the place of XF-MS amongst other structural biology methods and showcase some of the latest developments in its usage for studying water-mediated transmembrane signaling, ion transport and ligand-induced allosteric conformational changes in membrane proteins.

Keywords: hydroxyl-radical footprinting, oxidative labeling, mass spectrometry, ion channels, transporters, radiolysis

Introduction.

Membrane proteins, representing around 30% of all proteins in the genome, are crucial players in cellular sensory cascades and metabolite transport, and hence are prime pharmacological targets[1,2]. Elucidation of their functional mechanisms that could be exploited for therapeutic means relies on our detailed understanding of their structural transitions. However, membrane proteins have earned a deserved reputation of being difficult targets for structural investigation. While classical structure determination approaches such as crystallography and NMR provide high resolution information, they are limited in terms of sample preparation requirements (i.e. the necessity for crystallization, high protein concentrations, and/or non-physiological buffer conditions)[3-5]. Other structural techniques such as electron microscopy[6-8], small-angle scattering[9] and EPR[10] can provide novel structural information, but are limited in resolution, and are often conducted in non-natural environments. Recent advances in development of oxidative labeling techniques coupled with mass-spectrometric analysis of the data, provides an alternative and highly complementary approach to these more common structural tools, with the advantage of providing single residue resolution under near-physiological conditions[11]. In this review we describe the basic principles of oxidative labeling, its place relative to other mass-spectrometry based methods and its advantages in comparison to other available methods in application to membrane proteins and their complexes, as well as highlighting recent examples of its successful application. We also outline the latest developments and future promises of this exciting technology to study membrane protein structure and dynamics.

Part I: Comparison of different MS-based labeling approaches for study of protein structure and the role of oxidative labeling.

1.1 A brief history of footprinting approaches.

Footprinting as a technique has long been a staple of molecular biology. In a typical footprinting experiment, a control pattern of modification or degradation of a target macromolecule is compared with the pattern obtained in the presence of a partner molecule or a ligand, revealing differences resulting from conformational changes of the target or protection upon complex formation. Its usage for DNA both *in vivo* using dimethylsufate (DMS), a purine-methylating agent[12], or *in vitro* DNase I protection[13], goes back to the 70's.

Attempts to develop viable protein-protein interaction footprinting technology followed in the next couple of decades[14]. It was not, however, until the mid-90's that the first demonstration of the feasibility of using modification strategies to footprint proteins was made. Using a combination of both reversible and irreversible Lys-targeting agents and a Lys-specific endopeptidase, mapping of vaccinia virus topoisomease[15] was demonstrated. Nonetheless, these approaches remained rather laborious and ultimately did not gain traction, so almost another decade had to pass before advances in mass-spectrometry (MS) and proteomics finally allowed the development of several techniques capable of site-specific analysis of protein-protein interactions.

1.2. MS based approaches for studying protein-protein interactions.

For native proteins, MS is suitable for analysis of complexes, which are either very stable (e.g. immune complexes) or sampled using mild conditions – in what has become known as native MS[16]. Indeed, epitope mapping by MS is possible in antibody-antigen complexes, which are robust enough to survive MALDI deposition and desorption[17]. Individual epitopes can be identified by their respective ions' decreased signature in the antibody treated samples[18]. The majority of studied systems, however, are not stable enough for such approaches, and they are also not well adapted for the study of conformational dynamics or solvent accessibility, although introduction of MS-identifiable labels into the studied proteins can overcome these issues.

As a result, over the recent years, the fast development of mass-spectrometric methods has largely displaced proteolysis-based footprinting approaches. There are a number of different flavours of methods but in general they rely on attachment of a probe to the surface of the protein, and/or crosslinking with subsequent identification of the location of the label by MS-based sequencing of the protein following a proteolytic digest. One particularly noteworthy MS approach is based on the **usage of chemical cross-linkers** to identify local proximity of residues, either in a protein in isolation or following complex formation[19]. Guided by available crystal structures of proteins in isolation, this is a powerful technique, which can be used to map the interactions in large complexes. This approach, which has become known as **CLMS (cross-linking/mass-spectrometry**) has been successfully applied to the 180kDa Ndc complex[20], and a 15-subunit, 700kDa complex of RNA Pol II with TFIIF[21]. Cross-linking efficiency may differ, and ultimately is restricted by the availability of cross-linkable residues, typically Lys or Cys, depending on the type of the cross-linker. It is rather difficult to quantify the effects and provide time-resolved studies, although some progress has recently been achieved using isotope-labels[22].

An alternative method, also based on MS identification of the modification tags, is the usage of **isotope-coded affinity tag (ICAT)** reagents, which can be used to sample cysteine accessibility. ^{13}C labeled reactive tags (e.g. bromoacetamide) are first applied to natively folded proteins (including *in vivo* applications), following which ^{12}C tags are applied post-denaturation, allowing identification of accessible areas. Such ICAT footprinting was successfully used to map the surfaces of CheW that interact with the large multidomain histidine kinase CheA, as well as with the transmembrane chemoreceptor Tsr in native *E. coli* membranes[23].

Another powerful method based on MS usage is **H/D exchange (HD-X)**[24,25]. This is a reversible modification method, which relies on MS detection of deuterium in a studied peptide sequence as a result of exchange with amide hydrogen in the backbone of the target protein. Such exchange is only possible in solvent exposed regions and the speed of exchange can be correlated with the relative accessibility. A significant drawback of the method is the continuous exchange of the H/D that often cannot survive the required handling of the sample and/or purification.

1.3. Oxidative footprinting or hydroxyl radical footprinting.

As its name suggests, the **oxidative footprinting** approach relies on covalent modification (oxidation) of solvent accessible residues in proteins, which are subsequently identified by means of quantitative mass spectrometry. There are several ways to generate these radicals. One approach is based on **oxidative Fenton chemistry** using Fe (II)-EDTA[26], which was pioneered by Tullius & Dombrovski[26] for DNA footprinting. This oxidative cleavage approach was extended to protein mapping as demonstrated early on[27]. It has been commercialised under the name of **FeBABE** (referred to as "Iron Babe") (Pearce Biotechnology/Life Technologies), and uses Fe(III) (S)-1-(p-Bromoacetamido-benzyl)ethylene diamine tetraacetic acid as a sulfhydryl-reactive reagent that incorporates an Fe(III) EDTA moiety into a purified bait protein. The bromoacetyl group allows the reagent to attach covalently to sulfhydryl groups. When activated by ascorbate and peroxide, the Fe(III) EDTA group cleaves peptide bonds, acting as an artificial protease using oxidative Fenton chemistry. This technique has recently been successfully used in mapping the interactions within the large RNA Pol II pre-initiation complex[28], and has also recently been successfully adapted for *in vivo* application in bacterial cells[29,30].

Alternatively, the active hydroxyl radicals used for oxidative labeling can be generated using **laser photolysis** employing UV laser for dissociation of peroxide molecules [31,32]. This method has become known as **Fast photochemical oxidation of**

proteins (FPOP)[33]. Another method is actual generation of the oxidative species "on the fly" using electrospray MS with high needle voltages and oxygen as a reactive nebulizer[34].
However, the most popular currently employed approach is the **usage of ionizing radiation** for creating the active radicals from water, in a process that is known as **radiolysis**[35,36]. Radiolysis can be achieved using gamma rays[37], or high energy electrons[38]; however, it is prevalently achieved using high-density X-rays from synchrotron sources, and it is hence commonly known **as X-ray radiolytic footprinting or XRF**, or when paired with mass-spectrometric analysis, **XF-MS**. Both terms are used interchangeably from here on.

1.4. Basics on XRF.
Although using a different mechanism of generation of radicals, the principles of the XRF are essentially the same as other oxidative labeling approaches. To generate reactive hydroxyl radicals *in situ* a high brilliance flux of white-light photons (~10^{-15} per second) of varying energies in the 5-30 keV range is usually applied, although a monochromated beam can also be used[35,39]. The general reaction leading to generation of the reactive hydroxyl radicals in non-oxygenated solutions is the following:

$$2H_2O + e^- (h\nu \text{ ionising}) \rightarrow H_2O^{+\bullet} + H_2O^* + eaq^-$$

Where H_2O^* signifies excited water molecules. These excited molecules dissociate to hydroxyl radicals in less than 10^{-13} s, while the $H_2O^{+\bullet}$ reacts with another water molecule generating an additional hydroxyl radical:

$$H_2O^{+\bullet} + H_2O \rightarrow H_3O^+ + HO^{\bullet}$$

The general scheme of the typical XF-MS experiment is presented in **Figure 1**. In brief, a protein sample (in the micromolar range) is subjected to a short pulse of radiation using a microfluidic device or a fast kinetic setup such as KinTek[40], which causes oxidation events in the microsecond timeframe, following which the reaction is rapidly quenched using a reducing agent (e.g. methionine amide). The sample is then retrieved and is processed similar to any MS sample for proteomic analysis, with several steps that may include detergent removal, proteinase digestion and LC-MS/MS-MS identification of the fragments which have modifications. Experiments usually include a number of different exposure times, which are compared against a control, e.g. protein on its own *vs.* protein in the presence of a partner. Dose-response (DR) curves are calculated for each peptide fragment analysed, and the effective dose received is calibrated using internal references, such as Alexa[40]. Depending on the context, the detected differential labeling then can be attributed to conformational changes or interactions with partners [40,41].

Figure 1: General scheme for steady state and time resolved studies

In contract with soluble targets, membrane proteins are surrounded by a number of extrinsic •OH scavengers (cofactors, detergents, phospholipids) that reduce the effective dose to the protein[39]. An insufficient photon flux density requires longer time for delivery of the equivalent dose, which in turn increases secondary radiation damage, resulting in poor data quality and artifacts due to protein unfolding. In fact, XF studies on several membrane proteins were only possible at the NSLS footprinting beamline after the installation of a focusing mirror, which increased the useable flux density by 14 fold[42]. A short duration of high flux dose allows better structural integrity of the protein assembly and is a key factor in obtaining high quality data. The usage of pulsed beams makes it possible to limit radiation damage and the amount of hydroxyl radicals generated – typically between 0.2 to 3 μM in deaerated buffers – thus also ensuring that one-electron oxidized radical species and not two-electron oxidized forms are created[35,43]. The new XF facility at the ALS[39] and the upcoming XF beamline at NSLS II[44] are designed to provide the higher flux density that is necessary to allow investigation of complex integral membrane proteins and extend current beamline capabilities to the sub-millisecond timescale.
Laser photolysis and pulsed electron beams operate on the nanosecond timescale, allowing sampling of protein conformational dynamics in real time[31,32]. However, chemical or laser/H_2O_2 production of •OH relies on addition of reagents that can oxidize/damage and unfold proteins[38], as well as remove essential metal ions necessary for protein function[39]. In contrast, XF-MS is a straightforward technique in which the dose can simply be controlled by irradiation, permitting quantification of the reactivity rates of the modifiable sidechains. The most common variation utilizes a pulsed white synchrotron beam to which the sample is exposed on a millisecond or (with current advancements) microsecond timescale; however, monochromated beams can also be used[39]. One of the unique advantages of synchrotron-based XF-MS is that it has the ideal energy range (5-10 keV) to penetrate the sample solution and the cell membrane without severe perturbation to the protein. In addition, the high flux density provided by the latest generation of synchrotron sources has

the potential to reduce the irradiation time to submilliseconds and thus limit secondary damage to the protein. In contrast, in electron beam radiolysis (e.g. using a Van de Graaff generator), in which modifications are generated in submicroseconds, the energy deposition by 2 MeV electrons causes electron-induced protein damage[39]. Further technical aspects of radiolysis have been covered extensively elsewhere[39,41,43] and we will just highlight some of the advantages of the approach in the section below.

1.5. Advantages of XF in comparison to other methods.

In comparison to the other MS-based methods discussed above, the oxidative footprinting approach has a number of inherent advantages, e.g. it does not require any prior modification of the protein *via* mutagenesis or introduction of chemical labels, and unlike most of other label-based approaches, relies on the smallest possible probe – the hydroxyl radical, which is usually generated *in situ* in aqueous solutions close to physiological conditions.

Another major advantage of the technique is that it uses a relatively non-specific oxidation reaction, which affects most amino acid residues, given their proximity to a ionisable water molecule[11]. Thus, it is relatively independent of the protein sequence and it is also particularly effective in labeling hydrophobic and aromatic residues which are otherwise rather inert[11,45]. Importantly, it can be applied on the microsecond timescale, approaching the scale of conformational transitions in proteins, and in a time-resolved fashion allowing sampling of conformational dynamics in proteins. As a covalent modification method it also doesn't suffer from the issue of loss of signal and post-exposure artifactual labeling which is sometimes an issue with H/D-X. Oxidative labeling coupled to high-sensitivity MS also requires very little sample (nanogram amounts of protein) in comparison to many other structural biology techniques, which may be a major issue for difficult-to-obtain complexes and membrane targets. Perhaps most importantly, it provides direct information on the solvation state of a given residue and, as will be shown further below, on the role of bound water.

PART 2: Examples of usage of oxidative labeling in combination with MS for study of biological systems.

2.1 Complexes

The first successful application of oxidative footprinting in the study of protein complexes was in the calcium dependent interactions of actin-gelsolin[46], and calmodulin-mellitin[47]. In these studies, the radicals were generated *in situ* by coupling electrical discharges with electrospray MS. Soon after, pulsed X-ray radiolysis was used to reveal for the first time the interaction of actin with cofilin, highlighting the utility of the approach for studying difficult targets which are prone to polymerisation and hence difficult to handle by other structural approaches [48,49]. The method has since successfully tackled ambitious complex targets such as the acto-myosin complex[50]. Unlike most other structural biology methods, XF-MS is not limited by the size of the studied complex, and as such it is very well suited for analysis of multiprotein complexes, including megadalton assemblies such as the Clp proteasome[51] and even ribosome assemblies[52,53]. While these ribosomal studies are generally used to probe RNA conformational changes as opposed to protein-protein interactions, they are particularly significant because they represent an *in vivo* application of XRF.

Membrane protein complexes. The successes with soluble protein complexes paved the way for the usage of XF-MS for more challenging membrane protein targets such as photosystem II (PSII), responsible for the light induced water splitting and production of oxygen[54]. PSII functions as a dimeric supercomplex, each part of which contains 20 subunits. This study also validated the functional existence of the hypothesized water channels leading from the surface of the complex to the Mn_4O_5Ca cluster, which had been inferred from the high resolution structures of PS II[55]. Another recent radiolytic footprinting study that combined XF-MS with crosslinking[56] extended these findings by providing new insights into the dynamic aspects of the interaction between the components of PSII and demonstrating the crucial importance of water molecules, which are in fact an integral part of the protein. While these studies showcase the potential of XF-MS to the study of large membrane protein complexes, perhaps even more exciting than the ability of the technique to identify solvent channels and cavities within the membrane proteins is its unique ability to detect bound water.

2.2. Bound water detection in by XF-MS

Bound or structural waters are required for folding, stability, enzymatic activity and protein-protein interactions [57]. In particular, it has been shown that water has a significant role in forming the active site in a prototypical GPCR receptor, rhodopsin[58]. Moreover, a comparison of known GPCR structures revealed that water molecules in the hydrophobic core of these proteins interact with conserved residues, implying that these waters are probably as important for function as the conserved residues themselves[59], forming an integral part of the signal transduction cascade. In potassium channels, bound water was also shown to play a major role in their slow inactivation, while cavities inside transmembrane domains are formed by the interaction between bound water and amino acid residues [60].

Traditionally, water dynamics are explored using high-field NMR, such as nuclear Overhauser effect (NOE) and magnetic relaxation dispersion (MRD) methods. These techniques can indirectly calculate residence times of internal waters in proteins on the timescale of sub-nanoseconds to milliseconds[61-67]. However, our understanding of site-specific structural and

functional implications of bound water is limited due to lack of direct experimental evidence under near-physiological conditions and limitations of timescale for many exchange-competent technologies.
As shown earlier, XF-MS has the unique ability to generate local spurs of hydroxyl radicals that activate bound waters, which rapidly modify adjacent side chain groups, providing a direct probe of the local dynamics of functionally important amino acid residues on millisecond timescales[68], even in cavities insulated from external solvent. **Temperature dependent XF** allows differentiation between bound and bulk water interactions and has been successfully applied to small globular proteins such as cytochrome c and ubiquitin to identify bound water interactions on the surface and in cavities[68].
The recent development of time-resolved radiolytic labeling coupled to $H_2{}^{18}O$ exchange demonstrates that footprinting can probe the dynamics of residues adjacent to bound waters[68] (see **Figure 2**). This is based on the fact that the ^{18}O from the attacking hydroxyl radical remains attached to the **Met, Phe, Tyr, Trp, Cys** residues, while in other side chains the covalently attached oxygen is derived from a dissolved molecular oxygen[68].

Figure 2: General scheme for water exchange and labeling.

Unlike NMR approaches, this method is not limited by molecular size and sample concentration. However, the current time resolution is limited by the millisecond irradiation interval[68]. Ultra-fast continuous flow mixing devices are being developed, and in combination with the short pulse of intense X-rays available from the focused bending magnet sources at the ALS or the NSLSII, will allow monitoring of the time course of the dynamics of the exchange of bound water in and out of crevices, channels, ion pumps or membrane protein pores on microsecond timescales, contributing significantly to our understanding of ion-transport and ion gating [39,44].

2.3. XF-MS in the study of GPCRs

The conserved internal water network in the transmembrane domains of GPCRs participates in the transfer of signal from the chromophore or the agonist-binding site to allosteric sites ultimately regulating the G-protein activation for signal transduction[58]. In particular, in the photo-activation processes, which are well studied in the example of mammalian rhodopsin, studies demonstrated the involvement of transient intermediates leading to the so-called Meta II state that is competent for G-protein binding[69]. The available X-ray crystal structures of rhodopsin and its several photo-intermediates have dramatically increased our understanding of structural rearrangements upon the activation of GPCRs[69]. But it is also increasingly clear that static structures alone are not sufficient to provide a complete understanding of GPCR function, especially given the prominent role that is played by structural waters, which are only visible in very high resolution crystal structures, which are difficult to obtain for a number of membrane receptors. XF, on the other hand, has emerged as a novel approach to study GPCRs by *in situ* labeling of transmembrane (TM) residues located in proximity to bound water. The first molecular details of the photoactivation process came from the comparative XF studies of the dark state, meta II and opsin states from detergent-solubilised samples[59]. These results are summarized in **Figure 3**. Results indicated an increase in labeling efficiency near the retinal-binding region, conserved TM domains and in a few residues of cytoplasmic and extracellular loops upon activation. The local conformational changes arising from the isomerization of the covalently bound retinal appear to be propagated to the cytoplasmic surface by means of water reorganization, and rearrangement of the H-bonding network between bound water and amino-acid side chains in the TM domain as demonstrated by ^{18}O-labeled water exchange studies[59]. Combined XF and H/D-X experiments included the investigation of conformation changes due to the binding of heterotrimeric G-protein[69]. Monitoring the amount of $HO^{\bullet}$ radical-induced modification on rhodopsin, activated rhodopsin (meta II) and activated rhodopsin-G-protein allowed elucidation of the fine details of the dynamics of the internal water rearrangements that control the G-protein binding as well as location of the protein-protein interaction in both rhodopsin and G protein. This allowed XF-MS to be used to structurally validate a homology model for the 5-HT4R receptor, for which no high resolution structure was available[70], including predicted sites for internal water-side chain interaction, highlighting another important application of the XF-technology.

2.4. XF-MS applied to the study of K^+ ion channels

Ion channels present exceptionally good targets for study by XF-MS, as their activation and the associated channel "gating" events usually result in dramatic changes in water accessibility of the central pore of the channel which is, in the resting state, devoid of water, presenting a major energetic barrier to ion conduction[71]. In the case of potassium channels, these gating events are connected to a variety of regulatory stimuli and include several critical conformational transitions that are suggested to propagate from the inner side of the membrane, including the so-called bundle crossing[72], which is thought to be the principle gating mechanism for the majority of the K+ channels, and is absolutely required to be in an open conformation in order for the channel to be in a conductive state.
The study of the bundle crossing gating using crystallography proved to be challenging as the closed state appears to be energetically favourable resulting in channels preferentially crystallising in closed state[73,74], while their size precluded NMR analysis, leaving the question of structural transitions during gating unanswered for a number of years.

The first K-channel to be studied by XF-MS was KirBac 3.1[75], and the comparison of the closed state of the channel with an EDTA-induced opening revealed a dramatic increase in the solvent accessibility along the central cavity of the channel, as well as along the interface between the transmembrane (gating) domain and the cytoplasmic regulatory domain of the channel, and conformational transitions that were suggested to induce opening of the channel (**Figure 4)**. In addition, this study[75] highlighted the possibility of the presence of a hydrophobic gate in this inward rectifying potassium channel, namely the residue L124 which showed the highest level of change in accessibility between the two open and closed conformations of the channel. These predictions have been confirmed in full by the crystal structure of the open state of the channel[76]. Notably, although the existence of such hydrophobic gating for K-channels had been suggested much earlier[77], the XF-MS directly visualized the role of the L124 during the transition[78]. As hydrophobic gating is suggested to play a major role in a number of channels lacking traditional "bundle crossing gate", such as K2P channels and a number of other channels including pentameric ligand gated and the bacterial mechanoselective channels[71], XF-MS appears an ideally suited tool to interrogate the gating transitions in these channels in the future.
Similarly, during activation the pH-dependent bacterial KcsA channel undergoes gating at the bundle crossing with several charged residues suggested to play the role of proton sensors[79]. KcsA also possesses a unique C-terminal domain forming a cytoplasmic protrusion, which imposes steric limits on the bundle crossing gate and the contraction of which appears to control the opening of the channel and its inactivation[80]. The comparison of water accessibility between the wild type and non-inactivatable mutant E71A of KcsA enabled not only confirmation of the significant changes of the water accessibility of the C-terminal domain (Gupta, Chance, Tucker & Bavro *in preparation*) but also demonstrated radical changes in the solvent profiles of residues behind the selectivity filter of the channel which harbours the E71A mutation. These findings are consistent with the recent suggestion of the important role played by structured/bound water in stabilizing the conductive selectivity filter conformation[81] and highlights the potential of XF-MS for study of these systems.

2.5. XF-MS in the study of ion transporters

Developing an experimental approach that can monitor proton movements at the molecular level would have a major impact by providing valuable detailed understanding of structural and dynamic elements of the coupling mechanism by which the proton gradient is utilized to pump substrates against their concentration gradient by a number of secondary transporters. A recent study[82] capitalized on the unique capabilities of XF to investigate the mechanism of a prototypical proton-coupled Zn^{2+} transporter YiiP from the cytoplasmic membrane of *E. coli*. Intriguingly, the crystal structure of Zn-YiiP showed an absence of any polar residue that could carry the proton to the Zn binding or transport site and identified the presence of a hydrophobic barrier that divided the transport pathway between the intra- and extra-cellular cavity[83,84]. Comparative XF analysis on Zn^{2+}-bound and Apo-Yiip form identified functionally important residues adjacent to these cavities and also within the hydrophobic barrier, and showed that they undergo large, reciprocal water accessibility changes. In particular, the active site Zn-binding residue D49 (TM helix 2) and residue L152 forming part of the hydrophobic gate, located on TM helix 5 (TM5), showed a significant decrease in water accessibility upon zinc binding which is consistent with the available crystal structure of Zn-YiiP (**Figure 5)**. Zinc access to the transport-site appeared to shut off water access to L152, suggesting that L152 may function as an inter-cavity gate that controls alternating access of zinc ion and water molecules to the transport-site. In contrast, increased water accessibility changes were observed in several methionine residues located at the N- and C-terminus of TM5, which are either located on the opposite TM5 face (L152) or packed against the opposite TM5 face (including D49). This reciprocal change in water accessibility on two opposite faces of TM5 is consistent with its re-orientation in response to zinc binding, and provided a novel mechanism for zinc transport. In summary, XF-MS revealed that TM5 underwent a rigid-body re-orientation upon zinc binding and suggested that the release of zinc binding energy in the hydrophobic core might get transformed to mechanical energy to reorient TM5 and close the L152 gate.
This study highlights the potential of XF-MS for study of various membrane transporters, which would be of interest to the wider transporter community.

Conclusion:

Over the past decade, oxidative labeling, and more specifically its X-ray radiolytic footprinting (XF) variation has been developed into a nearly routine technique and has been applied to a diverse range of biological systems, yielding unique structural insights impossible to obtain by other structural methods[11,39,40,51,68,85-88]. Synchrotron-based XF has been used to elucidate structural changes within several membrane proteins, including G-protein coupled receptors[59,69,70], potassium channels[78], photosystem proteins[54,56,89] and ion transporters[82] associated with their activated or functional states. Availability of high resolution X-ray crystal structures of these proteins in the their ground state has validated the ability of the XF approach to determine plausible roles of transmembrane structural waters in the regulation of their functional states. Moreover, recent advancements in experimental strategies with high flux-density X-ray beams at synchrotron facilities[39] together with significant improvement in mass spectrometry-based data analysis methodologies[90,91], serve as an promising platform for the development of a unique, integrative structural method universally suited to study any membrane protein system. XF-MS is an ideal complement to both high- and low-resolution structural studies, e.g. allowing the accurate

placing of components within low-to-medium resolution maps from cryo-EM or solution scattering studies, while providing information on protein dynamics from static crystals structures. Thus, XF is a future-proof method, which requires very low protein sample concentrations, yields residue-specific information, and is able to provide both structural and protein-dynamics data with high degree of temporal resolution. Given the above, there is little doubt that XF-MS has the potential to become one of the most important tools in solving structural problems related to large complexes and membrane proteins.

References

1 Bakheet, T. M. & Doig, A. J. Properties and identification of human protein drug targets. *Bioinformatics* **25**, 451-457, doi:10.1093/bioinformatics/btp002 (2009).

2 Grimm, D. *et al.* Diagnostic and therapeutic use of membrane proteins in cancer cells. *Curr Med Chem* **18**, 176-190 (2011).

3 Carpenter, E. P., Beis, K., Cameron, A. D. & Iwata, S. Overcoming the challenges of membrane protein crystallography. *Current opinion in structural biology* **18**, 581-586, doi:10.1016/j.sbi.2008.07.001 (2008).

4 Hong, M., Zhang, Y. & Hu, F. Membrane protein structure and dynamics from NMR spectroscopy. *Annual review of physical chemistry* **63**, 1-24, doi:10.1146/annurev-physchem-032511-143731 (2012).

5 Ubarretxena-Belandia, I. & Stokes, D. L. Present and future of membrane protein structure determination by electron crystallography. *Advances in protein chemistry and structural biology* **81**, 33-60, doi:10.1016/B978-0-12-381357-2.00002-5 (2010).

6 Goldie, K. N. *et al.* Cryo-electron microscopy of membrane proteins. *Methods in molecular biology* **1117**, 325-341, doi:10.1007/978-1-62703-776-1_15 (2014).

7 Bartesaghi, A. & Subramaniam, S. Membrane protein structure determination using cryo-electron tomography and 3D image averaging. *Current opinion in structural biology* **19**, 402-407, doi:10.1016/j.sbi.2009.06.005 (2009).

8 Schmidt-Krey, I. Electron crystallography of membrane proteins: two-dimensional crystallization and screening by electron microscopy. *Methods* **41**, 417-426, doi:10.1016/j.ymeth.2006.07.011 (2007).

9 Breyton, C. *et al.* Small angle neutron scattering for the study of solubilised membrane proteins. *Eur Phys J E Soft Matter* **36**, 71, doi:10.1140/epje/i2013-13071-6 (2013).

10 Jeschke, G. DEER distance measurements on proteins. *Annual review of physical chemistry* **63**, 419-446, doi:10.1146/annurev-physchem-032511-143716 (2012).

11 Xu, G. & Chance, M. R. Hydroxyl radical-mediated modification of proteins as probes for structural proteomics. *Chemical reviews* **107**, 3514-3543 (2007).

12 Ogata, R. T. & Gilbert, W. An amino-terminal fragment of lac repressor binds specifically to lac operator. *Proc Natl Acad Sci U S A* **75**, 5851-5854 (1978).

13 Galas, D. J. & Schmitz, A. DNAse footprinting: a simple method for the detection of protein-DNA binding specificity. *Nucleic Acids Res* **5**, 3157-3170 (1978).

14 Rana, T. M. & Meares, C. F. N-Terminal Modification of Immunoglobulin Polypeptide Chains Tagged with Isothiocyanato Chelates. *Bioconjugate Chem* **1**, 357-362, doi:DOI 10.1021/bc00005a010 (1990).

15 Hanai, R. & Wang, J. C. Protein footprinting by the combined use of reversible and irreversible lysine modifications. *Proceedings of the National Academy of Sciences of the United States of America* **91**, 11904-11908 (1994).

16 Barrera, N. P. *et al.* Mass spectrometry of membrane transporters reveals subunit stoichiometry and interactions. *Nature methods* **6**, 585-587, doi:10.1038/nmeth.1347 (2009).

17 Kiselar, J. G. & Downard, K. M. Direct identification of protein epitopes by mass spectrometry without immobilization of antibody and isolation of antibody-peptide complexes. *Analytical chemistry* **71**, 1792-1801 (1999).

18 Morrissey, B. & Downard, K. M. A proteomics approach to survey the antigenicity of the influenza virus by mass spectrometry. *Proteomics* **6**, 2034-2041, doi:10.1002/pmic.200500642 (2006).

19 Rappsilber, J., Siniossoglou, S., Hurt, E. C. & Mann, M. A generic strategy to analyze the spatial organization of multi-protein complexes by cross-linking and mass spectrometry. *Analytical chemistry* **72**, 267-275 (2000).

20 Maiolica, A. *et al.* Structural analysis of multiprotein complexes by cross-linking, mass spectrometry, and database searching. *Mol Cell Proteomics* **6**, 2200-2211, doi:10.1074/mcp.M700274-MCP200 (2007).

21 Chen, Z. A. *et al.* Architecture of the RNA polymerase II-TFIIF complex revealed by cross-linking and mass spectrometry. *The EMBO journal* **29**, 717-726, doi:10.1038/emboj.2009.401 (2010).

22 Fischer, L., Chen, Z. A. & Rappsilber, J. Quantitative cross-linking/mass spectrometry using isotope-labelled cross-linkers. *J Proteomics* **88**, 120-128, doi:10.1016/j.jprot.2013.03.005 (2013).

23 Underbakke, E. S., Zhu, Y. & Kiessling, L. L. Protein footprinting in a complex milieu: identifying the interaction surfaces of the chemotaxis adaptor protein CheW. *J Mol Biol* **409**, 483-495, doi:10.1016/j.jmb.2011.03.040 (2011).

24 Konermann, L., Pan, J. & Liu, Y. H. Hydrogen exchange mass spectrometry for studying protein structure and dynamics. *Chem Soc Rev* **40**, 1224-1234, doi:10.1039/c0cs00113a (2011).

25 Wales, T. E. & Engen, J. R. Hydrogen exchange mass spectrometry for the analysis of protein dynamics. *Mass Spectrom Rev* **25**, 158-170, doi:10.1002/mas.20064 (2006).

26 Tullius, T. D. & Dombroski, B. A. Iron(II) EDTA used to measure the helical twist along any DNA molecule. *Science (New York, N.Y* **230**, 679-681 (1985).

27 Ermacora, M. R., Delfino, J. M., Cuenoud, B., Schepartz, A. & Fox, R. O. Conformation-dependent cleavage of staphylococcal nuclease with a disulfide-linked iron chelate. *Proceedings of the National Academy of Sciences of the United States of America* **89**, 6383-6387 (1992).

28 Grunberg, S., Warfield, L. & Hahn, S. Architecture of the RNA polymerase II preinitiation complex and mechanism of ATP-dependent promoter opening. *Nat Struct Mol Biol* **19**, 788-796, doi:10.1038/nsmb.2334 (2012).

29 Zhu, Y., Guo, T. & Sze, S. K. Elucidating structural dynamics of integral membrane proteins on native cell surface by hydroxyl radical footprinting and nano LC-MS/MS. *Methods Mol Biol* **790**, 287-303, doi:10.1007/978-1-61779-319-6_22 (2011).

30 Zhu, Y. *et al.* Elucidating in vivo structural dynamics in integral membrane protein by hydroxyl radical footprinting. *Mol Cell Proteomics* **8**, 1999-2010, doi:10.1074/mcp.M900081-MCP200 (2009).

31 Aye, T. T., Low, T. Y. & Sze, S. K. Nanosecond laser-induced photochemical oxidation method for protein surface mapping with mass spectrometry. *Analytical chemistry* **77**, 5814-5822, doi:10.1021/ac050353m (2005).

32 Hambly, D. M. & Gross, M. L. Laser flash photolysis of hydrogen peroxide to oxidize protein solvent-accessible residues on the microsecond timescale. *Journal of the American Society for Mass Spectrometry* **16**, 2057-2063, doi:10.1016/j.jasms.2005.09.008 (2005).

33 Zhang, H., Gau, B. C., Jones, L. M., Vidavsky, I. & Gross, M. L. Fast photochemical oxidation of proteins for comparing structures of protein-ligand complexes: the calmodulin-peptide model system. *Analytical chemistry* **83**, 311-318, doi:10.1021/ac102426d (2011).

34 Maleknia, S. D., Chance, M. R. & Downard, K. M. Electrospray-assisted modification of proteins: a radical probe of protein structure. *Rapid communications in mass spectrometry : RCM* **13**, 2352-2358, doi:10.1002/(SICI)1097-0231(19991215)13:23<2352::AID-RCM798>3.0.CO;2-X (1999).

35 Ralston, C. Y. *et al.* Time-resolved synchrotron X-ray footprinting and its application to RNA folding. *Methods in enzymology* **317**, 353-368 (2000).

36 Sclavi, B., Sullivan, M., Chance, M. R., Brenowitz, M. & Woodson, S. A. RNA folding at millisecond intervals by synchrotron hydroxyl radical footprinting. *Science* **279**, 1940-1943 (1998).

37 Ottinger, L. M. & Tullius, T. D. High-resolution in vivo footprinting of a protein-DNA complex using gamma-radiation. *J Am Chem Soc* **122**, 5901-5902, doi:DOI 10.1021/ja000285f (2000).

38 Watson, C. *et al.* Pulsed electron beam water radiolysis for submicrosecond hydroxyl radical protein footprinting. *Analytical chemistry* **81**, 2496-2505, doi:10.1021/ac802252y (2009).

39 Gupta, S., Celestre, R., Petzold, C. J., Chance, M. R. & Ralston, C. Development of a microsecond X-ray protein footprinting facility at the Advanced Light Source. *J Synchrotron Radiat* **21**, 690-699, doi:10.1107/S1600577514007000 (2014).

40 Gupta, S., Sullivan, M., Toomey, J., Kiselar, J. & Chance, M. R. The Beamline X28C of the Center for Synchrotron Biosciences: a national resource for biomolecular structure and dynamics experiments using synchrotron footprinting. *Journal of synchrotron radiation* **14**, 233-243, doi:10.1107/S0909049507013118 (2007).

41 Takamoto, K. & Chance, M. R. Radiolytic protein footprinting with mass spectrometry to probe the structure of macromolecular complexes. *Annu Rev Biophys Biomol Struct* **35**, 251-276, doi:10.1146/annurev.biophys.35.040405.102050 (2006).

42 Sullivan, M. R. *et al.* Installation and testing of a focusing mirror at beamline X28C for high flux x-ray radiolysis of biological macromolecules. *The Review of scientific instruments* **79**, 025101, doi:10.1063/1.2839027 (2008).

43 Houee-Levin, C. & Bobrowski, K. The use of the methods of radiolysis to explore the mechanisms of free radical modifications in proteins. *Journal of Proteomics* **92**, 51-62, doi:DOI 10.1016/j.jprot.2013.02.014 (2013).

44 Bohon, J., D'Mello, R., Ralston, C. Y., Gupta, S. & Chance, M. R. Synchrotron X-ray Footprinting on Tour. (2013).

45 Garrison, W. M. Reaction-Mechanisms in the Radiolysis of Peptides, Polypeptides, and Proteins. *Chemical reviews* **87**, 381-398, doi:DOI 10.1021/cr00078a006 (1987).

46 Maleknia, S. D. & Downard, K. Radical approaches to probe protein structure, folding, and interactions by mass spectrometry. *Mass spectrometry reviews* **20**, 388-401, doi:10.1002/mas.10013 (2001).

47 Wong, J. W. H., Maleknia, S. D. & Downard, K. M. Hydroxyl radical probe of the calmodulin-melittin complex interface by electrospray ionization mass spectrometry. *J Am Soc Mass Spectr* **16**, 225-233, doi:DOI 10.1016/j.jasms.2004.11.009 (2005).
48 Kamal, J. K., Benchaar, S. A., Takamoto, K., Reisler, E. & Chance, M. R. Three-dimensional structure of cofilin bound to monomeric actin derived by structural mass spectrometry data. *Proc Natl Acad Sci U S A* **104**, 7910-7915 (2007).
49 Guan, J. Q., Vorobiev, S., Almo, S. C. & Chance, M. R. Mapping the G-actin binding surface of cofilin using synchrotron protein footprinting. *Biochemistry* **41**, 5765-5775 (2002).
50 Oztug Durer, Z. A., Kamal, J. K., Benchaar, S., Chance, M. R. & Reisler, E. Myosin binding surface on actin probed by hydroxyl radical footprinting and site-directed labels. *Journal of molecular biology* **414**, 204-216, doi:10.1016/j.jmb.2011.09.035 (2011).
51 Bohon, J., Jennings, L. D., Phillips, C. M., Licht, S. & Chance, M. R. Synchrotron Protein Footprinting Supports Substrate Translocation by ClpA via ATP-Induced Movements of the D2 Loop. *Structure* **16**, 1157-1165 (2008).
52 Adilakshmi, T., Bellur, D. L. & Woodson, S. A. Concurrent nucleation of 16S folding and induced fit in 30S ribosome assembly. *Nature* **455**, 1268-1272, doi:10.1038/nature07298 (2008).
53 Clatterbuck Soper, S. F., Dator, R. P., Limbach, P. A. & Woodson, S. A. In vivo X-ray footprinting of pre-30S ribosomes reveals chaperone-dependent remodeling of late assembly intermediates. *Mol Cell* **52**, 506-516, doi:10.1016/j.molcel.2013.09.020 (2013).
54 Frankel, L. K. *et al.* Radiolytic mapping of solvent-contact surfaces in Photosystem II of higher plants: experimental identification of putative water channels within the photosystem. *The Journal of biological chemistry* **288**, 23565-23572, doi:10.1074/jbc.M113.487033 (2013).
55 Umena, Y., Kawakami, K., Shen, J. R. & Kamiya, N. Crystal structure of oxygen-evolving photosystem II at a resolution of 1.9 A. *Nature* **473**, 55-60, doi:10.1038/nature09913 (2011).
56 Mummadisetti, M. P. *et al.* Use of protein cross-linking and radiolytic footprinting to elucidate PsbP and PsbQ interactions within higher plant Photosystem II. *Proceedings of the National Academy of Sciences of the United States of America* **111**, 16178-16183, doi:10.1073/pnas.1415165111 (2014).
57 Ball, P. Water as an active constituent in cell biology. *Chem Rev* **108**, 74-108, doi:10.1021/cr068037a (2008).
58 Angel, T. E., Chance, M. R. & Palczewski, K. Conserved waters mediate structural and functional activation of family A (rhodopsin-like) G protein-coupled receptors. *Proc Natl Acad Sci U S A* **106**, 8555-8560, doi:10.1073/pnas.0903545106 (2009).
59 Angel, T. E., Gupta, S., Jastrzebska, B., Palczewski, K. & Chance, M. R. Structural waters define a functional channel mediating activation of the GPCR, rhodopsin. *Proceedings of the National Academy of Sciences of the United States of America* **106**, 14367-14372, doi:10.1073/pnas.0901074106 (2009).
60 Ostmeyer, J., Chakrapani, S., Pan, A. C., Perozo, E. & Roux, B. Recovery from slow inactivation in K+ channels is controlled by water molecules. *Nature* **501**, 121-124, doi:10.1038/nature12395 (2013).
61 Bertini, I., Huber, J. G., Luchinat, C. & Piccioli, M. Protein hydration and location of water molecules in oxidized horse heart cytochrome c by (1)H NMR. *J Magn Reson* **147**, 1-8 (2000).
62 Brunne, R. M., Liepinsh, E., Otting, G., Wuthrich, K. & van Gunsteren, W. F. Hydration of proteins. A comparison of experimental residence times of water molecules solvating the bovine pancreatic trypsin inhibitor with theoretical model calculations. *J Mol Biol* **231**, 1040-1048, doi:S0022-2836(83)71350-1 [pii]
10.1006/jmbi.1993.1350 (1993).
63 Denisov, V. P., Peters, J., Horlein, H. D. & Halle, B. Using buried water molecules to explore the energy landscape of proteins. *Nature structural biology* **3**, 505-509 (1996).
64 Nucci, N. V., Pometun, M. S. & Wand, A. J. Site-resolved measurement of water-protein interactions by solution NMR. *Nature structural & molecular biology* **18**, 245-249 (2011).
65 Otting, G., Liepinsh, E., Farmer, B. T., 2nd & Wuthrich, K. Protein hydration studied with homonuclear 3D 1H NMR experiments. *Journal of biomolecular NMR* **1**, 209-215 (1991).
66 Otting, G., Liepinsh, E. & Wuthrich, K. Protein hydration in aqueous solution. *Science (New York, N.Y* **254**, 974-980 (1991).
67 Persson, E. & Halle, B. Nanosecond to Microsecond Protein Dynamics Probed by Magnetic Relaxation Dispersion of Buried Water Molecules. *J. Am. Chem. Soc.* **130**, 1774-1787 (2008).
68 Gupta, S., D'Mello, R. & Chance, M. R. Structure and dynamics of protein waters revealed by radiolysis and mass spectrometry. *Proceedings of the National Academy of Sciences of the United States of America* **109**, 14882-14887, doi:10.1073/pnas.1209060109 (2012).
69 Orban, T. *et al.* Conformational dynamics of activation for the pentameric complex of dimeric G protein-coupled receptor and heterotrimeric G protein. *Structure* **20**, 826-840, doi:10.1016/j.str.2012.03.017 (2012).

70 Padayatti, P. S. *et al.* A hybrid structural approach to analyze ligand binding by the serotonin type 4 receptor (5-HT4). *Mol Cell Proteomics* **12**, 1259-1271, doi:10.1074/mcp.M112.025536 (2013).

71 Aryal, P., Sansom, M. S. & Tucker, S. J. Hydrophobic gating in ion channels. *J Mol Biol* **427**, 121-130, doi:10.1016/j.jmb.2014.07.030 (2015).

72 Swartz, K. J. Towards a structural view of gating in potassium channels. *Nat Rev Neurosci* **5**, 905-916, doi:10.1038/nrn1559 (2004).

73 Tao, X., Avalos, J. L., Chen, J. & MacKinnon, R. Crystal structure of the eukaryotic strong inward-rectifier K+ channel Kir2.2 at 3.1 A resolution. *Science* **326**, 1668-1674, doi:10.1126/science.1180310 (2009).

74 Uysal, S. *et al.* Crystal structure of full-length KcsA in its closed conformation. *Proceedings of the National Academy of Sciences of the United States of America* **106**, 6644-6649, doi:10.1073/pnas.0810663106 (2009).

75 Gupta, S. *et al.* Conformational Changes During the Gating of a Potassium Channel Revealed by Structural Mass Spectrometry. *Structure* **July**, In Press (2010).

76 Bavro, V. N. *et al.* Structure of a KirBac potassium channel with an open bundle crossing indicates a mechanism of channel gating. *Nature structural & molecular biology* **19**, 158-163, doi:10.1038/nsmb.2208 (2012).

77 Zimmerberg, J. & Parsegian, V. A. Polymer inaccessible volume changes during opening and closing of a voltage-dependent ionic channel. *Nature* **323**, 36-39, doi:10.1038/323036a0 (1986).

78 Gupta, S. *et al.* Conformational changes during the gating of a potassium channel revealed by structural mass spectrometry. *Structure* **18**, 839-846, doi:10.1016/j.str.2010.04.012 (2010).

79 Thompson, A. N., Posson, D. J., Parsa, P. V. & Nimigean, C. M. Molecular mechanism of pH sensing in KcsA potassium channels. *Proceedings of the National Academy of Sciences of the United States of America* **105**, 6900-6905, doi:10.1073/pnas.0800873105 (2008).

80 Uysal, S. *et al.* Mechanism of activation gating in the full-length KcsA K+ channel. *Proceedings of the National Academy of Sciences of the United States of America* **108**, 11896-11899, doi:10.1073/pnas.1105112108 (2011).

81 Raghuraman, H., Islam, S. M., Mukherjee, S., Roux, B. & Perozo, E. Dynamics transitions at the outer vestibule of the KcsA potassium channel during gating. *Proceedings of the National Academy of Sciences of the United States of America* **111**, 1831-1836, doi:10.1073/pnas.1314875111 (2014).

82 Gupta, S. *et al.* Visualizing the kinetic power stroke that drives proton-coupled zinc(II) transport. *Nature* **512**, 101-104, doi:10.1038/nature13382 (2014).

83 Lu, M. & Fu, D. Structure of the zinc transporter YiiP. *Science.* **317**, 1746-1748. (2007).

84 Lu, M., Chai, J. & Fu, D. Structural basis for autoregulation of the zinc transporter YiiP. *Nat Struct Mol Biol* **16**, 1063-1067 (2009).

85 Kiselar, J. G. & Chance, M. R. Future directions of structural mass spectrometry using hydroxyl radical footprinting. *Journal of mass spectrometry : JMS* **45**, 1373-1382, doi:10.1002/jms.1808 (2010).

86 Klinger, A. L. *et al.* A synchrotron-based hydroxyl radical footprinting analysis of amyloid fibrils and prefibrillar intermediates with residue-specific resolution. *Biochemistry* **53**, 7724-7734, doi:10.1021/bi5010409 (2014).

87 Kiselar, J. G., Datt, M., Chance, M. R. & Weiss, M. A. Structural analysis of proinsulin hexamer assembly by hydroxyl radical footprinting and computational modeling. *The Journal of biological chemistry* **286**, 43710-43716, doi:10.1074/jbc.M111.297853 (2011).

88 Kamal, J. K. & Chance, M. R. Modeling of protein binary complexes using structural mass spectrometry data. *Protein Sci* **17**, 79-94, doi:ps.073071808 [pii]
10.1110/ps.073071808 (2008).

89 Leverenz, R. L. *et al.* A 12 Å carotenoid translocation in a photoswitch associated with cyanobacterial photoprotection. *Science* **In press** (2015).

90 Kaur, P., Kiselar, J., Yang, S. & Chance, M. R. Quantitative Protein Topography Analysis and High-Resolution Structure Prediction Using Hydroxyl Radical Labeling and Tandem-Ion Mass Spectrometry (MS). *Mol Cell Proteomics* **14**, 1159-1168, doi:10.1074/mcp.O114.044362 (2015).

91 Kaur, P., Kiselar, J. G. & Chance, M. R. Integrated algorithms for high-throughput examination of covalently labeled biomolecules by structural mass spectrometry. *Analytical chemistry* **81**, 8141-8149, doi:10.1021/ac9013644 (2009).

Figure Captions:

Figure 1: Schematic diagram of X-ray footprinting using synchrotron radiolysis and mass spectrometry. The example illustrates the labelling protection in a protein domain resulting from a conformational change from state A to state B. Following the X-ray irradiation on a (sub)microsecond timescale to generate surface modification at solvent accessible sites, reaction is quenched immediately by methionine amide and digested with specific proteases. Resulting peptide fragments are analyzed by reverse phase liquid chromatography coupled with mass spectrometry (LC-MS), which separates out the peptides and quantitatively determines the extent of modification at irradiation point. Specific sites of modification are determined by mass spectrometry sequence analysis (MS/MS). The fractions of unmodified peptide vs. exposure time (dose-response or DR-plot) provide site-specific modification rate constants *(k sec $^{-1}$)*. The rates are compared among different sample conditions, and their ratios (R), which are independent of intrinsic reactivity, account for the degree in solvent accessibility changes due to any conformational changes/interactions. The final results can be mapped into available structures or used as constraints for Structural Modeling.

Figure 2: Schematic diagram of time-resolved radiolytic ^{18}O-labeling and water exchange. (A) Rapid mixing combined with ^{18}O-mediated hydroxyl radical labeling allows to monitor the time-course of exchange of water in protein. LC-MS is used to identify and isolate the modified peptides, targeted MS/MS is used to identify the sites of ^{18}O-labeling, and higher resolution isotopic distribution (zoom scan) is used to quantify the ratio of ^{18}O vs. ^{16}O labeling at various mixing delays. (B) Reaction schemes for the incorporation of ^{18}O in Phe where a direct addition of to OH• to aromatic ring results in a resonance-delocalized radical, which, following an addition of O_2, is rearomatized by elimination of hydroperoxyl ion. Following this mechanism, the final product retains the O-atom from the original OH•. Thus, upon irradiating solutions containing $H_2{}^{18}O$, ^{18}OH• is generated, which selectively labels Phe residues giving rise to +18 Da modification products. The Tyr, Trp, Met, and Cys can be ^{18}O labeled by a similar mechanism. (C) Examples of a zoom-scan for singly protonated peptide. The most abundant peak indicates the position of the monoisotopic mass of the ^{16}O-adduct; the peaks shifted by 2 m⁄z units from this mass contain a mixture of the ^{18}O monoisotopic mass and the (two) ^{13}C containing ^{16}O isotope. The decreased abundance at this m⁄z value relative to the monotisotopic mass, for 50% vs. 97% $H_2{}^{18}O$, is indicated by an arrow and represents the potential signal for an exchange experiment. (C) Progress curves (circles and error bars) of water exchange for the ^{18}O labeled side-chain residues. The solid line represents the single exponential function fit, which determines the residence time of bound water in proximity of a side chain.

Figure 3: Pictorial summary of relative solvent accessibility changes for the photoactivation of dark rhodopsin to Meta II state. Residues with rate constants $>0.1s^{-1}$ are rendered as sticks and colored by the ratio of rate constants between Meta-II and Rhodopsin. Conserved transmembrane waters are shown in cyan spheres. The changes in rates of modification reflect local structural changes upon formation of Meta II. The result demonstrates disruption and reorganization of multiple close-packing interactions, mediated by both side chains and bound waters. The information is transmitted from the chromophore (ligand-binding site) to the cytoplasmic surface for G-protein activation.

Figure 4: Mapping the solvent accessibility changes from close to open conformation in KirBac3.1. Modified residues are represented by sticks on the X-ray crystal structure of close KirBac3.1 (PDB-1XL4). Subunits are represented by different colours. SH, TM1, PH, TM2 denotes Slide Helix, Transmembrane helix 1 (Outer Helix), Pore Helix and Transmembrane (Inner) Helix 2; respectively. The color codes indicate the changes in the modification rates or solvent accessibilities upon transition from close to the open state. Residues in KirBac3.1 that have increased interactions with solvent due to changes in the structure of the channel in the open state have dramatically increased labeling efficiency in comparison to their rate of modification in the closed state.

Figure 5: X-ray footprinting reveals a hydrophobic gate at residue L152, which controls the opening of inner cavity water pathway for zinc-proton exchange in YiiP transporter. Cross-sectional view shows the position of TM helices, which separate out two cavities at the intra-cellular (IC) and extra-cellular (EC) side. (A) Residues coloured in red and blue showed an increase and decrease in the solvent accessibility in response to zinc binding respectively. The XF results suggest the protein conformational change alternates the membrane-facing on–off mode of zinc coordination (in D49) and protonation–deprotonation (H153) of the transport site in a coordinated fashion. (B) The view of the proposed water pathway, which connects EC with IC after excluding the residue L152 from the surface drawing of the TM helices.

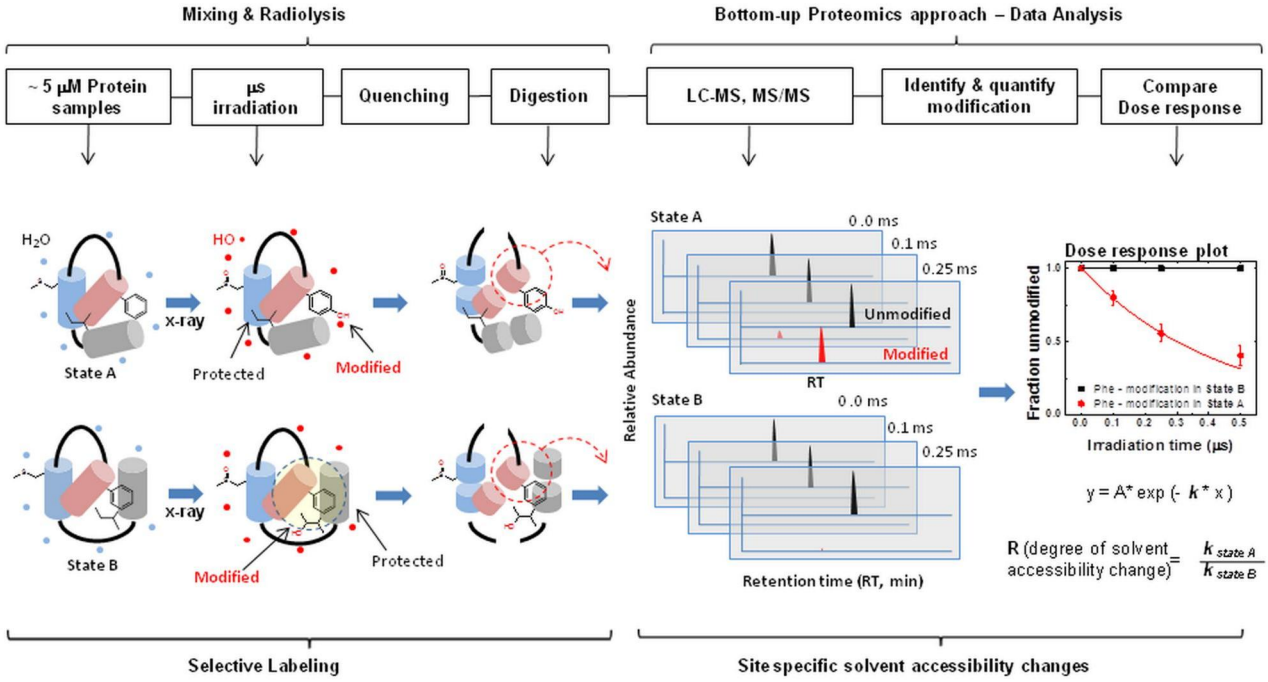
Mixing & Radiolysis
Bottom-up Proteomics approach – Data Analysis
~ 5 µM Protein samples
µs irradiation
Quenching
Digestion
LC-MS, MS/MS
Identify & quantify modification
Compare Dose response
H2O
HO•
X-ray
State A
Protected
Modified
State B
Modified
Protected
Relative Abundance
State A
0.0 ms
0.1 ms
0.25 ms
Unmodified
Modified
RT
State B
0.0 ms
0.1 ms
0.25 ms
Retention time (RT, min)
Dose response plot
Fraction unmodified
Phe - modification in State B
Phe - modification in State A
Irradiation time (µs)
y = A* exp (- k * x)
R (degree of solvent accessibility change) = k state A / k state B
Selective Labeling
Site specific solvent accessibility changes

Figure 1

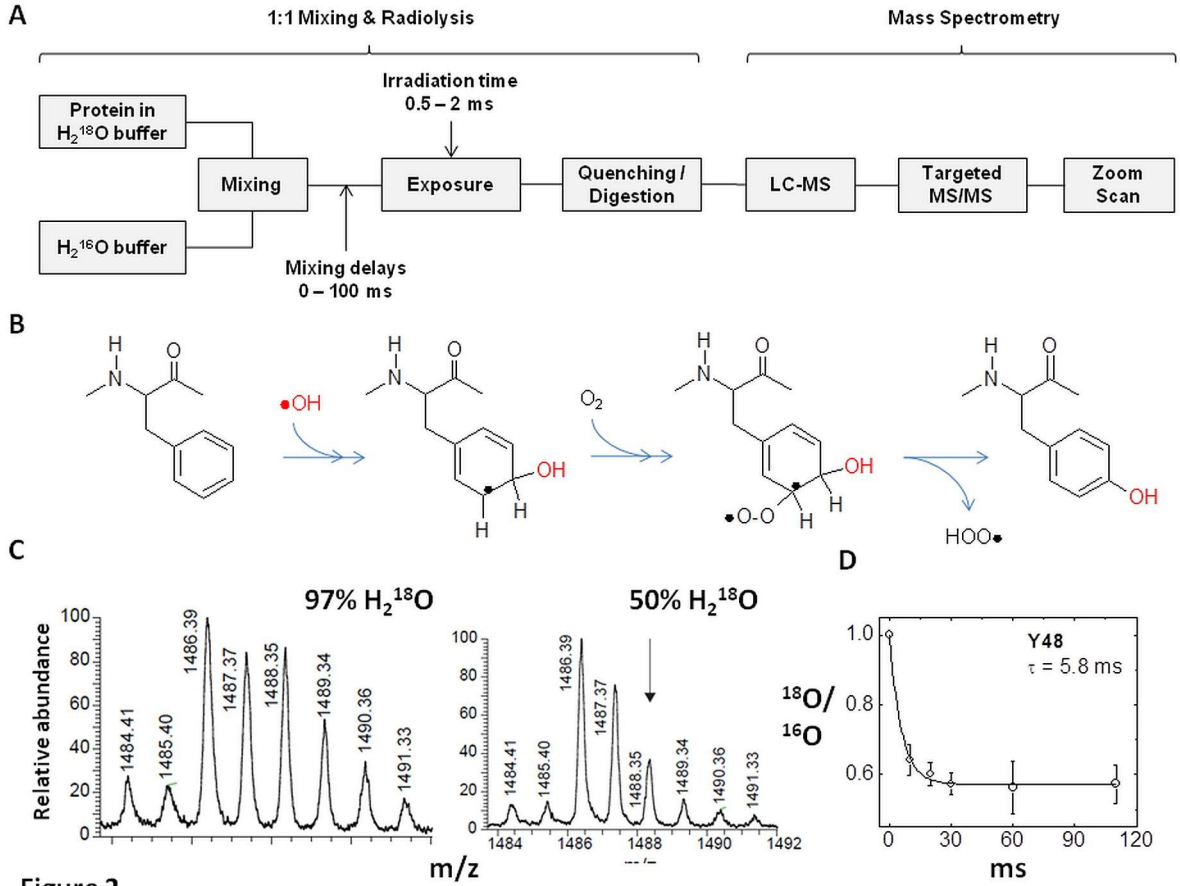
A
1:1 Mixing & Radiolysis
Mass Spectrometry
Irradiation time
0.5 – 2 ms
Protein in
H2 18O buffer
H2 16O buffer
Mixing
Exposure
Quenching /
Digestion
LC-MS
Targeted
MS/MS
Zoom
Scan
Mixing delays
0 – 100 ms
B
•OH
O2
OH
H
O-O
HOO•
C
97% H2 18O
50% H2 18O
Relative abundance
m/z
1484.41
1485.40
1486.39
1487.37
1488.35
1489.34
1490.36
1491.33
D
18O/
16O
Y48
τ = 5.8 ms
ms

Figure 2

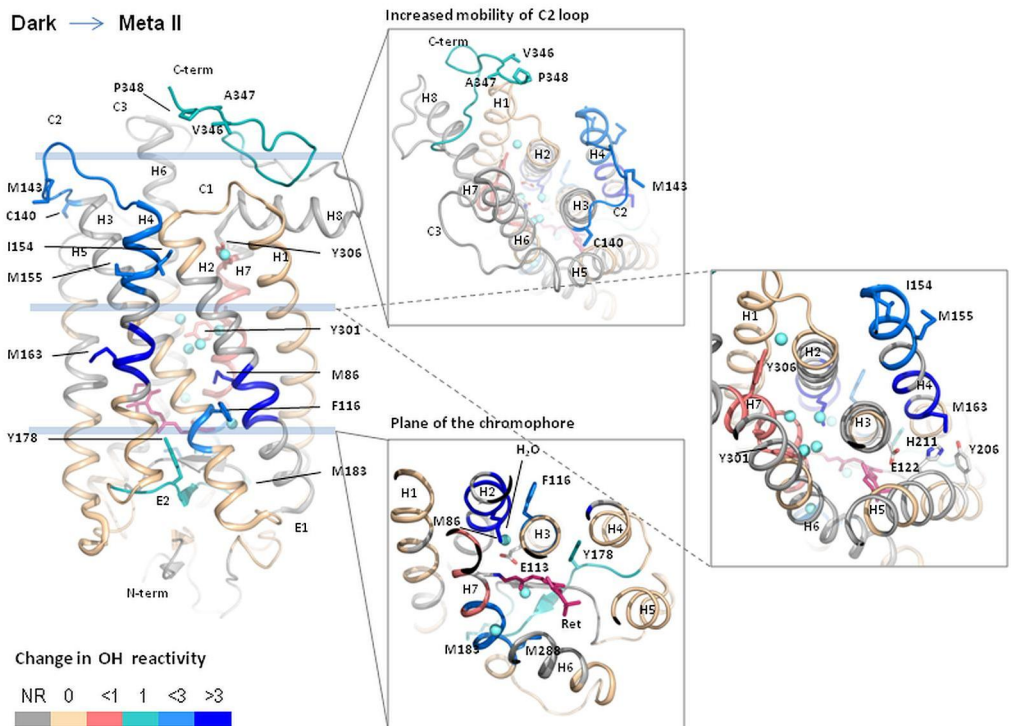
Dark → Meta II
C-term
P348
A347
C3
V346
C2
H6
M143
C1
C140
H3
H4
H8
I154
H5
H1
Y306
M155
H2
H7
Y301
M163
M86
F116
Y178
M183
E2
E1
N-term
Change in OH reactivity
NR 0 <1 1 <3 >3
Increased mobility of C2 loop
C-term
V346
A347
P348
H8
H1
H2
H4
M143
H7
H3
C2
C3
H6
C140
H5
Plane of the chromophore
H2O
F116
H1
H2
M86
H3
H4
Y178
E113
H7
H5
Ret
M183
M288
H6
I154
H1
M155
H2
Y306
H4
H7
M163
H3
H211
Y206
Y301
E122
H5
H6

Figure 3

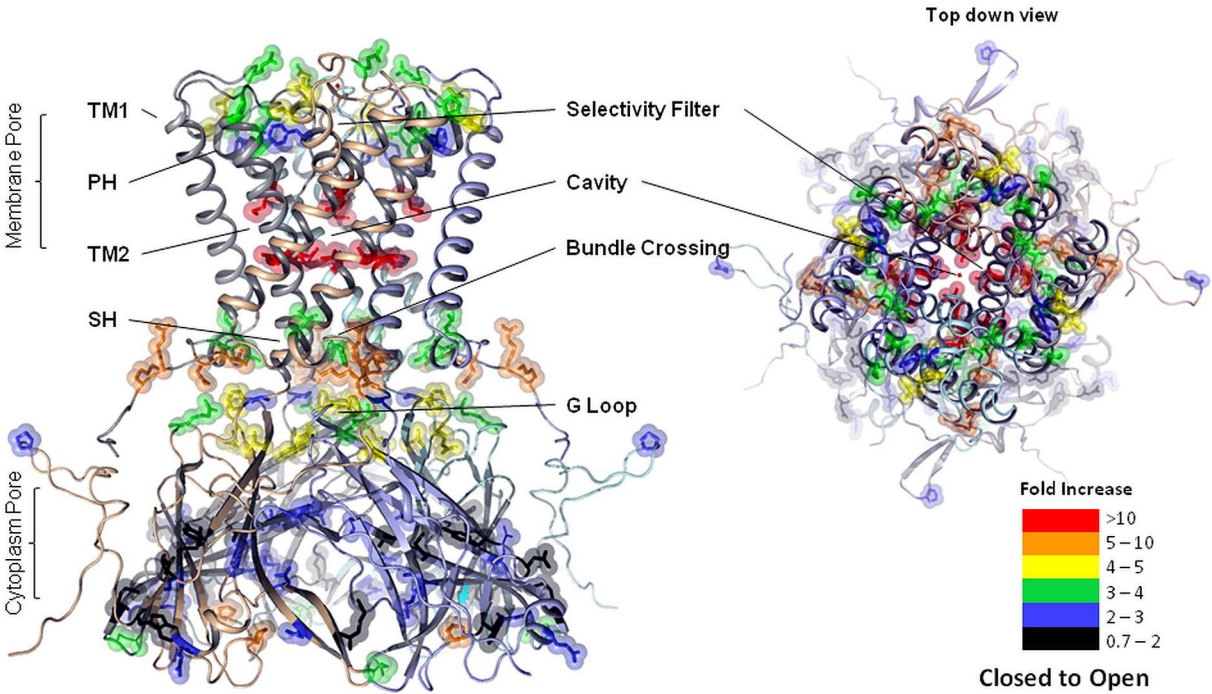
Top down view
TM1
PH
TM2
SH
Membrane Pore
Cytoplasm Pore
Selectivity Filter
Cavity
Bundle Crossing
G Loop
Fold Increase
>10
5 – 10
4 – 5
3 – 4
2 – 3
0.7 – 2
Closed to Open

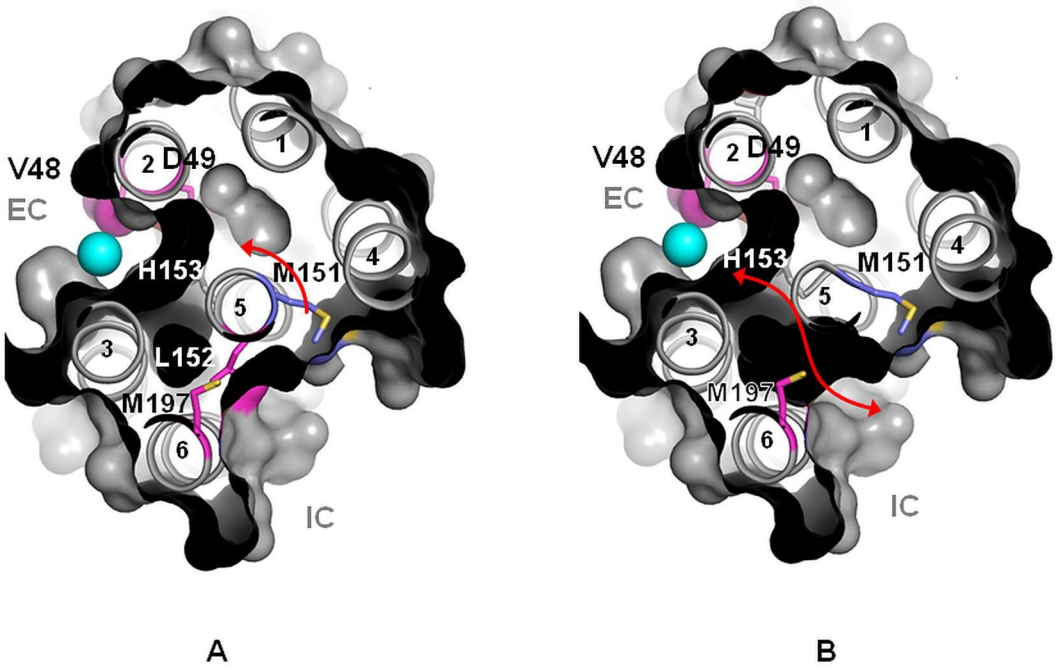
V48
EC
2 D49
1
H153
M151
4
5
3
L152
M197
6
IC
A
V48
EC
2 D49
1
H153
M151
4
5
3
M197
6
IC
B

Figure 5